Reactions of Early Lanthanide Metal Atoms (Nd, Sm, Eu) with Water Molecules. A Matrix Isolation Infrared Spectroscopic and Theoretical Study

Jia Xu and Mingfei Zhou*

Department of Chemistry and Laser Chemistry Institute, Shanghai Key Laboratory of Molecular Catalysts and Innovative Materials, Fudan University, Shanghai 200433, P. R. China

Received: June 17, 2006; In Final Form: July 25, 2006

The reactions of early lanthanide metal atoms Nd, Sm, and Eu with water molecules have been investigated using matrix isolation infrared spectroscopy and density functional calculations. The reaction intermediates and products were identified on the basis of isotopic labeled experiments and density functional frequency calculations. The ground state metal atoms react with water to form the $M(H_2O)$ and $M(H_2O)_2$ complexes spontaneously on annealing (M = Nd, Sm, Eu). The $M(H_2O)$ complexes isomerize to the inserted HMOH molecules under red light irradiation, which further decompose to give the metal monoxides upon UV light irradiation. The $Nd(H_2O)_2$ complex decomposes to form the trivalent $HNd(OH)_2$ molecule, while the $Sm(H_2O)_2$ and $Eu(H_2O)_2$ complexes rearrange to the divalent $Sm(OH)_2$ and $Eu(OH)_2$ molecules under red light irradiation.

Introduction

The interactions of metal centers with water molecules are of interest in a wide variety of areas, such as catalytic synthesis, surface chemistry, and biochemical systems. The reactions of metal atoms, ions, and clusters with water serve as the simple models for understanding the reactivity pattern of more complicated systems. Previous experimental and theoretical studies have provided a wealth of insight concerning the reactivity and mechanism of transition metal atoms and ions with water molecules.[1−13] It was found that early transition metal atoms and ions reacted with water to form the metal monoxide neutrals and cations in the gas phase.[1−5] Matrix isolation infrared spectroscopic studies showed that early transition metal atoms reacted with water molecules to form initially the HMOH insertion intermediates spontaneously on annealing.[7−11] The insertion molecules could either photochemically isomerize to the high valent H_2MO molecules or decompose to the metal monoxide and H_2.[7,9,10] The later transition metal atoms reacted with water to give the $M(H_2O)$ complexes, which rearranged to the insertion products under UV−visible light excitation.[8,11]

The reactions of f element metals with water have also gained some attention, but largely on the actinide metals.[14−18] The reaction of uranium cation with water were investigated in the gas phase. Two reaction channels leading to UO^+ and UOH^+ were observed.[14−16] Matrix isolation infrared spectroscopic studies indicate that the neutral thorium and uranium atoms directly insert into the O−H bond of water to form the H_2ThO and H_2UO species.[17,18] In recent years, lanthanide coordination complexes in aqueous solution have gained considerable interest in molecular recognition and chirality sensing of biological substrate. A large number of lanthanide−water complexes have been structurally characterized.[19] To have a fundamental understanding of the reactivities of lanthanide metal with water, we performed a comprehensive matrix isolation infrared spectroscopic and theoretical study of the reactions of lanthanide metal atoms with water. In this paper, we first report the results on early lanthanide metal atoms, Nd, Sm, and Eu. Various reaction intermediates and products are identified, and the reaction mechanisms are discussed.

Experimental and Theoretical Methods

The experiment for pulsed laser evaporation and matrix isolation infrared spectroscopic investigation is similar to those used previously.[20] Briefly, a Nd:YAG laser fundamental (1064 nm, 10 Hz repetition rate with 10 ns pulse width) was focused onto the rotating metal targets. The laser-evaporated metal atoms were co-deposited with water in excess argon onto a CsI window cooled normally to 6 K by means of a closed-cycle helium refrigerator (ARS, 202N). The matrix gas deposition rate was typically 4 mmol per hour. The H_2O/Ar mixtures were prepared in a stainless steel vacuum line using standard manometric technique. Distilled water was cooled to 77 K using liquid N_2 and evacuated to remove volatile impurities. Isotopic labeled D_2O and $H_2{}^{18}O$ (Cambridge Isotopic Laboratories) were used without further purification. Isotopic exchange with water adsorbed on the walls of the vacuum line occurred readily; in the experiments with D_2O sample, the HDO and H_2O absorptions were also presented. After sample deposition, IR spectra were recorded on a Bruker IFS66V spectrometer at 0.5 cm^{-1} resolution using a liquid nitrogen cooled HgCdTe (MCT) detector for the spectral range of 4000−400 cm^{-1}. Samples were annealed at different temperatures and subjected to broad band irradiation using a tungsten lamp or a high-pressure mercury arc lamp with glass filters.

Quantum chemical calculations were performed to determine the molecular structures and to help the assignments of vibrational frequencies of the observed reaction products. The calculations were performed at the level of density functional theory (DFT) with the B3LYP method, where the Becke three-parameter hybrid functional and the Lee−Yang−Parr correlation functional were used.[21] The 6-311++G** basis sets were used for the H and O atoms, and the scalar-relativistic SDD pseudopotential and basis sets were used for the Nd, Sm, and Eu

* To whom correspondence should be addressed. E-mail: mfzhou@fudan.edu.cn.

10.1021/jp063776g CCC: $33.50
Published on Web 08/23/2006

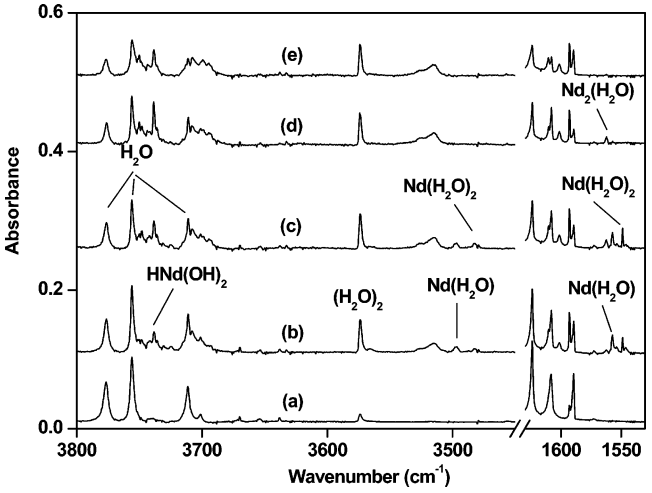

Figure 1. Infrared spectra in the 3800−3450 and 1630−1530 cm^{-1} regions from co-deposition of laser-evaporated Nd atoms with 0.2% H_2O in argon: (a) 1 h of sample deposition at 6 K; (b) after 20 K annealing; (c) after 25 K annealing; (d) after 15 min of $\lambda > 500$ nm irradiation; and (e) after 15 min of $250 < \lambda < 580$ nm irradiation.

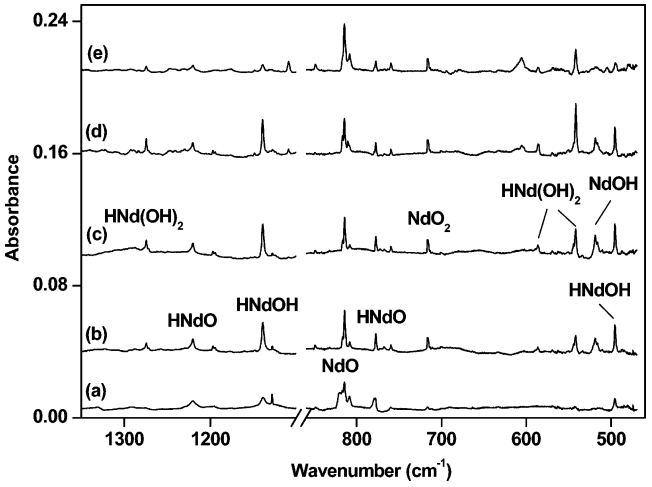

Figure 2. Infrared spectra in the 1350−1100 and 860−460 cm^{-1} regions from co-deposition of laser-evaporated Nd atoms with 0.2% H_2O in argon: (a) 1 h of sample deposition at 6 K; (b) after 20 K annealing; (c) after 25 K annealing; (d) after 15 min of $\lambda > 500$ nm irradiation; and (e) after 15 min of $250 < \lambda < 580$ nm irradiation.

atoms.[22,23] Geometries were fully optimized, and vibrational frequencies were calculated with analytical second derivatives. These DFT calculations were performed using the Gaussian 03 program.[24]

Results and Discussion

Infrared Spectra. A series of experiments has been done using different H_2O concentrations (ranging from 0.05% to 0.2% in argon) and relatively low laser energies (5−10 mJ/pulse). At such experimental conditions, atomic metal reactions dominate the chemistry, and no obvious dimetal or trimetal species were identified. The representative infrared spectra in selected regions using the Nd target with a 0.2% H_2O in argon sample are illustrated in Figures 1 and 2, respectively, and the product absorptions are listed in Table 1. On the basis of their growth/decay characteristics measured as a function of changes of experimental conditions, the observed product absorptions can be classified into several groups. The 3496.8 and 1557.2 cm^{-1} absorptions formed very weakly on sample deposition, increased on 20 K annealing, but decreased upon higher temperature annealing, and disappeared when the matrix was irradiated by the output of a tungsten lamp with a $\lambda > 500$ nm pass filter. The 3482.7 and 1548.8 cm^{-1} absorptions appeared when the matrix was annealed to 20 K, markedly increased on subsequent higher temperature annealing, and were totally bleached on $\lambda > 500$ nm irradiation. The 1139.0 and 495.5 cm^{-1} absorptions are weak upon sample deposition, increased on sample annealing and on $\lambda > 500$ nm irradiation, but decreased significantly upon continued irradiation with the output of a high-pressure mercury arc lamp ($250 < \lambda < 580$ nm). Four absorptions at 3738.4, 1274.4, 586.5, and 541.9 cm^{-1} increased together on sample annealing and on $\lambda > 500$ nm irradiation, but decreased upon $250 < \lambda < 580$ nm irradiation. The intensities of the 3496.8, 1557.2, 3482.7, and 1548.8 cm^{-1} absorptions decreased whereas the intensities of the 1139.0, 495.5, 3738.4, 1274.4, 586.5, and 541.9 cm^{-1} absorptions increased with increasing the sample scan times, which imply that the red irradiation from the IR spectrometer can readily induce isomerization reactions. In addition, weak absorptions at 1220.2 and 777.5 cm^{-1} were observed on sample deposition and kept almost unchanged upon annealing and different wavelength range irradiation; a weak absorption at 518.7 cm^{-1} appeared on sample annealing and disappeared under red light irradiation. Absorptions of NdO (814.5 cm^{-1}) and NdO_2 (717.0 cm^{-1}) were observed.[25] The NdO absorption slightly increased upon $\lambda > 500$ nm irradiation, and increased more upon $250 < \lambda < 580$ nm irradiation. The NdO_2 absorptions are mainly from trace of dioxygen impurity.

TABLE 1: Infrared Absorptions (cm^{-1}) from Co-Deposition of Laser-Evaporated Nd Atoms with H_2O in Excess Argon

			assignment	
H_2O	D_2O	$H_2{}^{18}O$	molecule	mode
3738.4			$HNd(OH)_2$	asym OH str
3496.8		3489.4	$Nd(H_2O)$	sym HOH str
3482.7		3475.6	$Nd(H_2O)_2$	HOH str
1557.2	1155.4	1550.7	$Nd(H_2O)$	H_2O bending
1548.8	1149.1	1542.3	$Nd(H_2O)_2$	asym H_2O bending
1562.3	1158.9	1555.7	$Nd_2(H_2O)$	H_2O bending
1274.4	912.9	1274.2	$HNd(OH)_2$	Nd−H str
1220.2	879.0	1219.8	HNdO	Nd−H str
1139.0	814.5	1138.6	HNdOH	Nd−H str
777.5	772.6	738.2	HNdO	Nd−O str
586.5			$HNd(OH)_2$	sym Nd−OH str
541.9		518.4	$HNd(OH)_2$	asym Nd−OH str
518.7	509.6	495.5	NdOH	Nd−OH str
495.5	484.3	472.7	HNdOH	Nd−OH str

Similar experiments were also performed using the Sm and Eu metal targets. Infrared spectra from co-deposition of laser-evaporated Sm with 0.2% H_2O in argon gave four groups of product absorptions as shown in Figures 3 and 4. The band positions are listed in Table 2. The 3505.1 and 1560.3 cm^{-1} group appeared on sample deposition, increased on annealing, and disappeared upon $\lambda > 500$ nm irradiation. The 3479.0 and 1547.7 cm^{-1} group appeared on sample annealing and exhibited similar annealing and irradiation behaviors as observed with the 3505.1 and 1560.3 cm^{-1} absorptions. The 1154.7 and 495.4 cm^{-1} absorptions are broad on sample deposition, sharpened when the sample was annealed to 20 K, slightly decreased upon sample annealing to 25 K, increased under $\lambda > 500$ nm irradiation, but decreased on continued $250 < \lambda < 580$ nm irradiation. The final group appeared at 462.1 and 488.0 cm^{-1}, increased on sample annealing and on $\lambda > 500$ nm irradiation, and kept almost unchanged upon $250 < \lambda < 580$ nm irradiation. Very similar infrared spectra were observed when the Sm target was replaced by the Eu target. Figures 5 and 6 show the Eu + H_2O

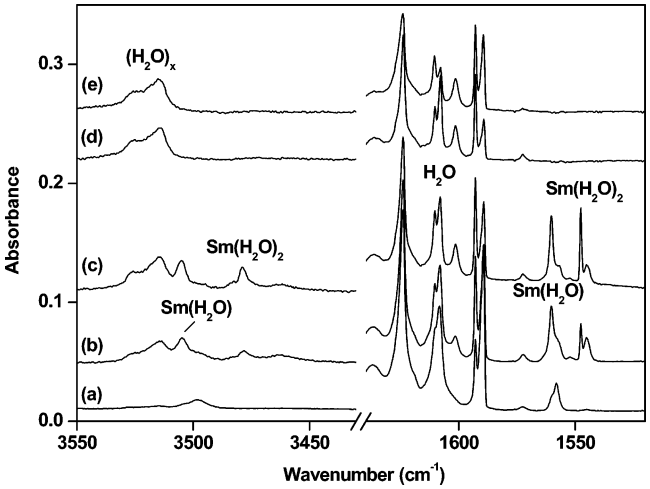

Figure 3. Infrared spectra in the 3550−3430 and 1640−1520 cm^{-1} regions from co-deposition of laser-evaporated Sm atoms with 0.2% H_2O in argon: (a) 1 h of sample deposition at 6 K; (b) after 20 K annealing; (c) after 25 K annealing; (d) after 15 min of $\lambda > 500$ nm irradiation; and (e) after 15 min of $250 < \lambda < 580$ nm irradiation.

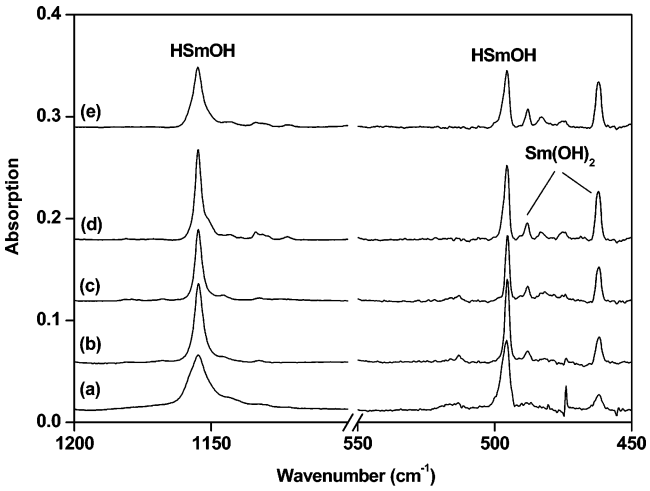

Figure 4. Infrared spectra in the 1200−1100 and 550−450 cm^{-1} regions from co-deposition of laser-evaporated Sm atoms with 0.2% H_2O in argon: (a) 1 h of sample deposition at 6 K; (b) after 20 K annealing; (c) after 25 K annealing; (d) after 15 min of $\lambda > 500$ nm irradiation; and (e) after 15 min of $250 < \lambda < 580$ nm irradiation.

TABLE 2: Infrared Absorptions (cm^{-1}) from Co-Deposition of Laser-Evaporated Sm Atoms with H_2O in Excess Argon

			assignment	
H_2O	D_2O	$H_2{}^{18}O$	molecule	mode
3505.1	2574.3	3498.3	$Sm(H_2O)$	sym HOH str
3479.0	2558.8	3472.0	$Sm(H_2O)_2$	HOH str
1560.3	1157.1	1553.8	$Sm(H_2O)$	H_2O bending
1547.7	1148.3	1541.1	$Sm(H_2O)_2$	asym H_2O bending
1154.7	824.8	1154.7	HSmOH	Sm−H str
495.4	484.9	472.2	HSmOH	Sm−OH str
488.0	478.0		$Sm(OH)_2$	sym SmOH str
462.1	452.2	441.2	$Sm(OH)_2$	asym SmOH str

spectra in selected regions, and Table 3 lists the observed frequencies.

Isotopic labeled $H_2{}^{18}O$, D_2O, and $H_2{}^{16}O + H_2{}^{18}O$ mixture were employed for product identification through isotopic shifts and splittings. The isotopic counterparts are also listed in Tables 1−3. The spectra in selected regions using different isotopic samples are shown in Supporting Information (Figures S1−S6).

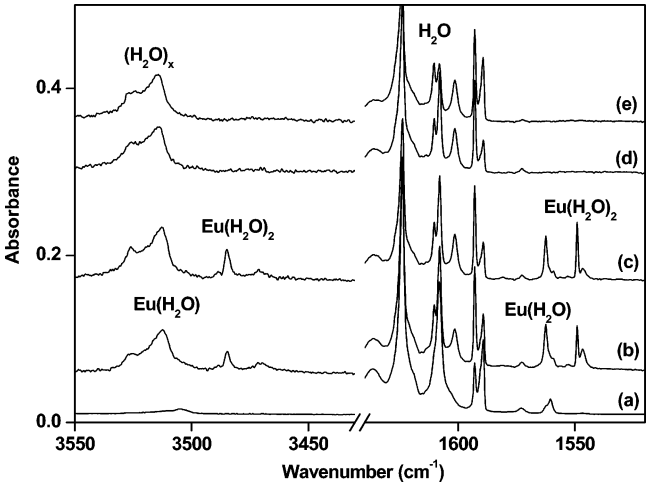

Figure 5. Infrared spectra in the 3550−3430 and 1640−1520 cm^{-1} regions from co-deposition of laser-evaporated Eu atoms with 0.2% H_2O in argon: (a) 1 h of sample deposition at 6 K; (b) after 20 K annealing; (c) after 25 K annealing; (d) after 15 min of $\lambda > 500$ nm irradiation; and (e) after 15 min of $250 < \lambda < 580$ nm irradiation.

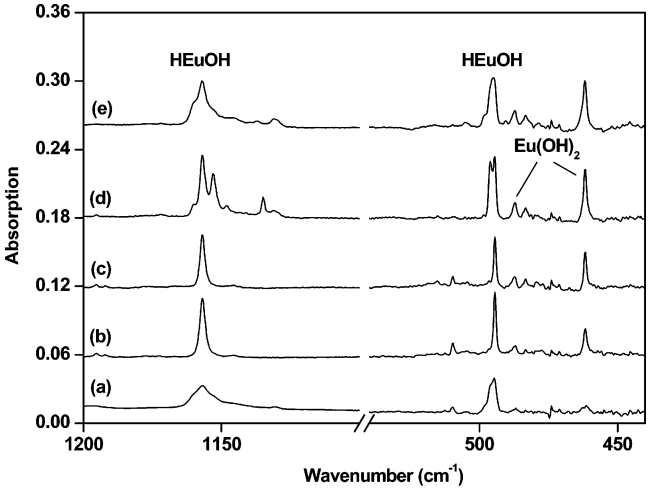

Figure 6. Infrared spectra in the 1200−1100 and 540−440 cm^{-1} regions from co-deposition of laser-evaporated Eu atoms with 0.2% H_2O in argon: (a) 1 h of sample deposition at 6 K; (b) after 20 K annealing; (c) after 25 K annealing; (d) after 15 min of $\lambda > 500$ nm irradiation; and (e) after 15 min of $250 < \lambda < 580$ nm irradiation.

TABLE 3: Infrared Absorptions (cm^{-1}) from Co-Deposition of Laser-Evaporated Eu Atoms with H_2O in Excess Argon

			assignment	
H_2O	D_2O	$H_2{}^{18}O$	molecule	mode
3510.8		3505.0	$Eu(H_2O)$	sym HOH str
3484.8		3477.5	$Eu(H_2O)_2$	HOH str
1562.5		1556.3	$Eu(H_2O)$	H_2O bending
1549.0		1542.4	$Eu(H_2O)_2$	asym H_2O bending
1157.0	826.9	1156.5	HEuOH	Eu−H str
494.4	484.4	471.3	HEuOH	Eu−OH str
487.1		462.6	$Eu(OH)_2$	sym EuOH str
461.7	451.5	440.9	$Eu(OH)_2$	asym EuOH str

M(H_2O). The 1557.2 cm^{-1} absorption in the Nd + H_2O reaction shifted to 1550.7 cm^{-1} with $H_2{}^{18}O$, and to 1155.4 cm^{-1} with D_2O, giving an isotopic $^{16}O/^{18}O$ ratio of 1.0042 and a H/D ratio of 1.3478. The band position and isotopic shifts are characteristic of the H_2O bending vibration of a H_2O complex perturbed by one metal atom. In the experiment when a $H_2{}^{16}O + H_2{}^{18}O$ mixed sample was used, no intermediate absorptions were observed, which confirms that only one H_2O subunit is involved

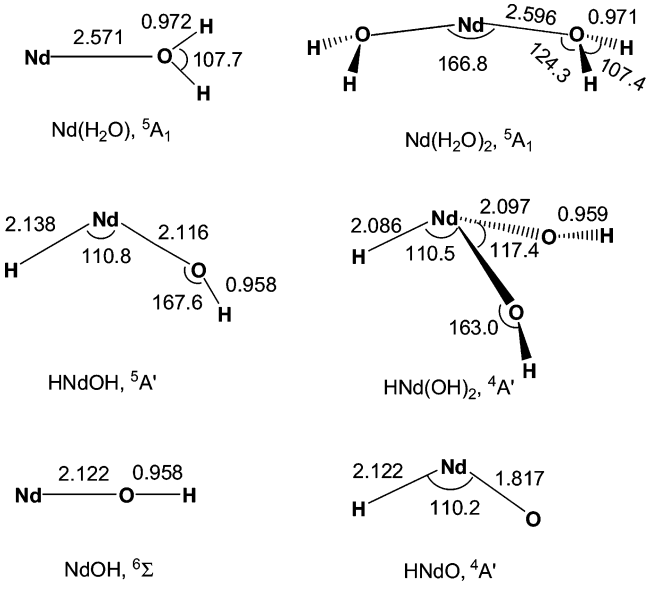

Figure 7. Optimized geometries (bond lengths in angstrom, bond angles in degree) of various products for the Nd + H_2O reactions.

in this complex. Accordingly, the 1557.2 cm^{-1} absorption is assigned to the Nd(H_2O) complex. An associate weak absorption at 3496.8 cm^{-1} is due to the symmetric HOH stretching vibration of the complex.

DFT calculations indicate that the Nd(H_2O) complex has a planar C_{2v} structure with a quintet ground state, as shown in Figure 7. The Nd−O distance was predicted to be 2.571 Å. The symmetric HOH stretching and H_2O bending vibrational frequencies were computed at 3621.5 and 1577.2 cm^{-1}, respectively, which are quite close to the experimental frequencies. The calculated isotopic frequency ratios are also in quite good agreement with the experimental values (Table 4). The antisymmetric HOH stretching vibration was predicted at 3730 cm^{-1} with zero IR intensity. At the B3LYP level, the Nd(H_2O) complex has a $^5A_1$ ground state with an electron configuration of (core) $(5b_1)^1$ $(2a_2)^1$ $(5b_2)^1$ $(10a_1)^1$ $(11a_1)^2$, which correlates to the $f^4d^0s^2$ ground state of the Nd atom.

Similar absorptions at 1560.3 and 3505.1 cm^{-1} in the Sm + H_2O experiments, and 1562.5 and 3510.8 cm^{-1} in the Eu + H_2O experiments, are assigned to the symmetric HOH stretching and H_2O bending vibrations of the Sm(H_2O) and Eu(H_2O) complexes, respectively. Both complexes were predicted to have planar structure with C_{2v} symmetry (Figure 8). The Sm(H_2O) complex has a $^7A_2$ ground state, and the Eu(H_2O) complex has a $^8A_2$ ground state. The experimentally observed vibrations were computed at 3628.6 and 1579.5 cm^{-1} for Sm(H_2O) and at 3633.0 and 1582.4 cm^{-1} for Eu(H_2O), respectively (Tables 5 and 6).

M(H_2O)$_2$. Absorptions at 1548.8 and 3482.7 cm^{-1} in the Nd + H_2O reaction favored high H_2O concentration experiments and increased on higher temperature annealing at the expense of the Nd(H_2O) absorptions. These experimental observations suggest that the 1548.8 and 3482.7 cm^{-1} absorptions involve more than one H_2O molecule. The low mode shifted to 1149.1 cm^{-1} with D_2O and to 1542.3 cm^{-1} with $H_2{}^{18}O$. The band position and isotopic frequency ratios are indicative of the H_2O bending vibration of a H_2O complex. The 3482.7 cm^{-1} absorption is due to the HOH stretching mode of the complex. In the experiment with equimolar mixture of $H_2{}^{16}O$ and $H_2{}^{18}O$, a triplet at 1548.8, 1544.1, and 1542.3 cm^{-1} was clearly resolved for the low mode. This spectral feature indicates that the complex involves two equivalent H_2O subunits and, therefore, are assigned to the Nd(H_2O)$_2$ complex.

The Nd(H_2O)$_2$ complex was calculated to have a $^5A_1$ ground state with C_{2v} symmetry (Figure 7). The Nd−O distance is 2.596 Å, slightly longer than that of Nd(H_2O). The ∠ONdO is 166.8°. The $^5A_1$ ground state also correlates to the $f^4d^0s^2$ ground state of the Nd atom. The two experimentally observed vibrations were computed at 3638.8 and 1575.6 cm^{-1}, respectively.

The absorptions at 1547.7 and 3479.0 cm^{-1} in the Sm + H_2O experiments are assigned to the Sm(H_2O)$_2$ complex, which was predicted to have a $^7A_2$ ground state. The 1549.0 and 3484.8 cm^{-1} in the Eu + H_2O experiments are assigned to the Eu(H_2O)$_2$ complex in its $^8A_2$ ground state. The calculated vibrational frequencies and isotopic frequencies ratios (Tables 5 and 6) support the experimental assignments.

With a water concentration of 0.2% in argon, water aggregates formed readily on sample annealing; however, no evidence was found for the formation of higher M(H_2O)$_x$ ($x \geq 3$) complexes in the experiments. This experimental observation suggests that the maximum coordination number of Nd, Sm, and Eu atoms is two with respect to water in solid argon. Consistent with that notion, the Nd(H_2O)$_3$ complex was predicted to be unbound with respect to Nd(H_2O)$_2$ + H_2O. The coordination of only two water molecules for neutral lanthanide metal atoms is quite different with the lanthanide metal cations, which can coordinate up to nine water molecules.[19] It is well-known that water ligand is a σ donor, but not a π acceptor. The move of water charge to the neutral metal atom results in negative charge accumulation on the metal center, which prevents further water coordination. In contrast, the lanthanide cations (Ln^{3+}) are highly electron deficient and are able to accept more donations from water ligands than the neutral atoms.

HMOH. Absorptions at 1139.0 and 495.5 cm^{-1} in the Nd + H_2O reaction are assigned to the HNdOH molecule. The upper mode showed very small shift (0.4 cm^{-1}) with $H_2{}^{18}O$. The deuterium counterpart was overlapped by the NdO absorption at 814.5 cm^{-1}. The band position and isotopic shifts indicate that the upper mode is a typical Nd−H stretching vibration.[26] The low mode shifted to 484.3 cm^{-1} with D_2O and to 472.7 cm^{-1} with $H_2{}^{18}O$ and is due mainly to a Nd−OH stretching mode. The mixed $H_2{}^{16}O$ + $H_2{}^{18}O$ spectra indicate that only one O atom is involved, while the mixed H_2O + HDO + D_2O spectra indicate that two inequivalent H atoms are involved in the mode. The HNdOH molecule was predicted to have a $^5A'$ ground state. The Nd−H and Nd−OH stretching vibrations were calculated to be 1153.0 and 510.9 cm^{-1}.

In the reaction of Sm and H_2O, similar absorptions at 1154.7 and 495.4 cm^{-1} are assigned to the Sm−H and Sm−OH stretching vibrations of the HSmOH molecule. DFT calculations predicted the HSmOH molecule to have a $^7A''$ ground state with Sm−H and Sm−OH stretching frequencies at 1184.3 and 510.3 cm^{-1}, respectively, which agree well with the experimental values. The absorptions at 1157.0 and 494.4 cm^{-1} in the Eu + H_2O reaction are assigned to the Eu−H and Eu−OH stretching vibrations of the HEuOH molecule. This molecule was predicted to have a $^8A''$ ground state. The two experimentally observed modes were calculated at 1193.1 and 514.5 cm^{-1} with isotopic frequency ratios also in reasonable agreement with the experimental values (Table 6).

M(OH)$_2$ (M = Sm, Eu). In the reaction of Sm with H_2O, two absorptions at 488.0 and 462.1 cm^{-1} showed the same annealing and photolysis behavior and are due to different vibrational modes of the same molecule. These two absorptions exhibit about the same isotopic frequency ratios (Table 2), which are suggestive of Sm−OH stretching vibrations. The mixed $H_2{}^{16}O$ + $H_2{}^{18}O$ and H_2O + HDO + D_2O spectra clearly indicate

TABLE 4: Calculated Vibrational Frequencies (cm^{-1}) and Isotopic Frequency Ratios of the Nd + H_2O Reaction Products[a]

		freq		H/D		$^{16}O/^{18}O$	
molecule	mode	calcd	obsd	obsd	calcd	obsd	calcd
$Nd(H_2O)$	sym HOH str	3621.5	3496.8	−	1.3880	1.0021	1.0021
	H_2O bending	1577.2	1557.2	1.3478	1.3624	1.0042	1.0046
$Nd(H_2O)_2$	HOH str	3638.8	3482.7	−	1.3877	1.0020	1.0021
	H_2O bending	1575.6	1548.8	1.3478	1.3630	1.0042	1.0045
HNdO	Nd−H str	1264.6	1220.2	1.3882	1.4008	1.0003	1.0002
	Nd−O str	821.0	777.5	1.0063	1.0053	1.0532	1.0538
NdOH	Nd−OH str	522.7	518.7	1.0179	1.0265	1.0468	1.0507
HNdOH	Nd−H str	1153.0	1139.0	1.3984	1.4075	1.0004	1.0000
	Nd−OH str	510.9	495.5	1.0231	1.0338	1.0482	1.0480
$HNd(OH)_2$	asym OH str	3925.4	3738.4	−	1.3731	−	1.0033
	Nd−H str	1335.7	1274.4	1.3960	1.4070	1.0002	1.0002
	sym Nd−OH str	579.6	586.5	−	1.0300	−	1.0513
	asym Nd−OH str	543.4	541.9	−	1.0317	1.0453	1.0462

[a] The experimental frequencies and ratios are also listed for comparison.

that two equivalent OH subunits are involved in these vibrations. Accordingly, we assign the 488.0 and 462.1 cm^{-1} absorptions to the symmetric and antisymmetric Sm−OH stretching vibrations of the $Sm(OH)_2$ molecule. As shown in Figure 8, the $Sm(OH)_2$ molecule was predicted to have a $^7A_2$ ground state. The ground state has a planar C_{2v} structure with ∠OSmO = 123.2°. The linear structure was predicted to lie 4.9 kcal/mol higher in energy than the bent structure and is a transition state with an imaginary frequency. The symmetric and antisymmetric Sm−OH stretching vibrations of the ground state molecule were calculated at 493.8 and 475.3 cm^{-1} with the calculated isotopic frequency ratios in quite good agreement with the experimental values (Table 5). The symmetric and antisymmetric O−H stretching modes were predicted at 3931.2 and 3931.9 cm^{-1}. The IR intensities of these two modes are lower than those of the Sm−OH stretching modes (Table S2). These two modes

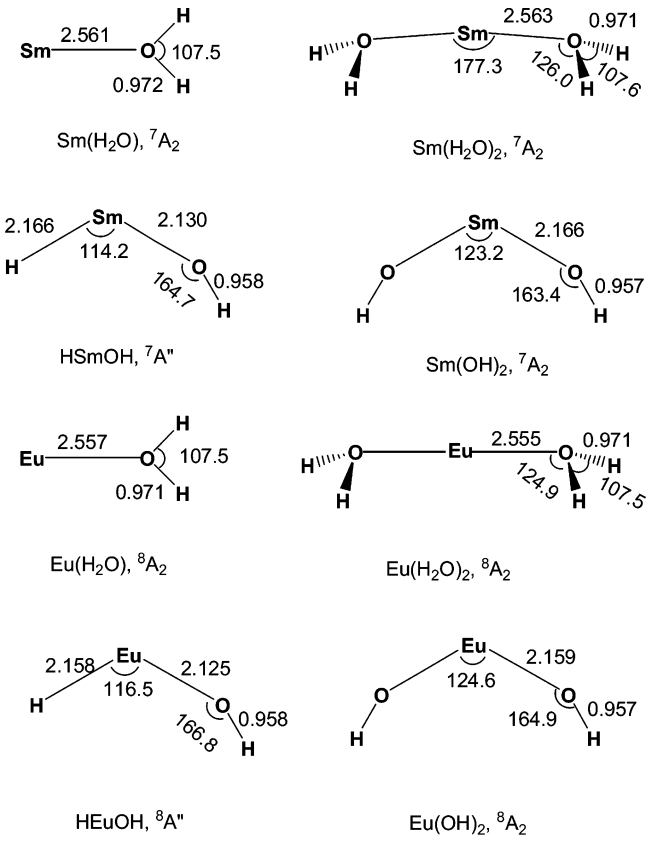

Figure 8. Optimized geometries (bond lengths in angstrom, bond angles in degree) of various products for the Sm + H_2O and Eu + H_2O reactions.

are not observed due to weakness or being overlapped by the strong water absorptions.

Similar absorptions at 487.1 and 461.7 cm^{-1} in the Eu and H_2O experiments are assigned to the symmetric and antisymmetric Eu−OH stretching vibrations of the $Eu(OH)_2$ molecule. DFT calculations predicted that the $Eu(OH)_2$ molecule has a $^8A_2$ ground state (Figure 8) with the symmetric and antisymmetric Eu−OH stretching frequencies at 503.4 and 481.3 cm^{-1}, respectively.

$HNd(OH)_2$. No evidence was found for the formation of $Nd(OH)_2$ molecule in the Nd + H_2O experiments. DFT calculations predicted that $Nd(OH)_2$ has a $^5A_1$ ground state. The most intense IR absorption is the antisymmetric Nd−OH stretching vibration at 485.0 cm^{-1}, ca. 25.9 cm^{-1} lower than the Nd−OH stretching mode of HNdOH. However, four absorptions at 3738.4, 1274.4, 586.5, and 541.9 cm^{-1} were observed which can be grouped together by their consistent behavior upon annealing and photolysis. The 3738.4 cm^{-1} absorption is due to an O−H stretching vibration. The 1274.4 cm^{-1} absorption exhibits very small shift with $H_2{}^{18}O$, but shifted to 912.9 cm^{-1} with D_2O. The band position and isotopic shifts imply that this absorption is due to a Nd−H stretching vibration. The spectral feature in the experiment with the $H_2O/HDO/D_2O$ mixture indicates that only one Nd−H bond is involved. The 586.5 and 541.9 cm^{-1} absorptions fall into the Nd−OH stretching frequency region. In the experiment with equimolar mixture of $H_2{}^{16}O$ and $H_2{}^{18}O$, a triplet at 541.9, 525.9, and 518.4 cm^{-1} was clearly resolved for the low mode, which indicates that two equivalent OH subunits are involved in the molecule. The above-mentioned experimental observations suggest the assignment of the four absorptions to the $HNd(OH)_2$ molecule. The $HNd(OH)_2$ molecule was calculated to have a nonplanar $^4A'$ ground state (Figure 7). The experimentally observed vibrations were calculated at 3925.4, 1335.7, 579.6, and 543.4 cm^{-1}, respectively.

Other Absorptions. In the Nd + H_2O experiments, two absorptions at 1220.2 and 777.5 cm^{-1} were observed on sample deposition. The 1220.2 cm^{-1} band shifted to 879.0 cm^{-1} with D_2O (H/D ratio of 1.3882) and is due to a Nd−H stretching vibration. The 777.5 cm^{-1} absorption exhibited an isotopic $^{16}O/^{18}O$ ratio of 1.0542, which is very close to the diatomic NdO ratio. The band position and isotopic ratios imply that this band is a terminal Nd−O stretching vibration.[25] This mode is weakly coupled by one H atom. The 777.5 cm^{-1} absorption shifted to 772.6 cm^{-1} with D_2O. The 1220.2 and 777.5 cm^{-1} absorptions are assigned to the HNdO molecule, which was predicted to have a $^4A'$ ground state (Figure 7). The Nd−H and Nd−O stretching vibrational frequencies were computed at 1264.6 and 821.0 cm^{-1} (Table 4).

TABLE 5: Calculated Vibrational Frequencies (cm^{-1}) and Isotopic Frequency Ratios of the Sm + H_2O Reaction Products[a]

		freq		H/D		$^{16}O/^{18}O$	
molecule	mode	calcd	obsd	obsd	calcd	obsd	calcd
$Sm(H_2O)$	sym HOH str	3628.6	3505.1	1.3616	1.3880	1.0019	1.0020
	H_2O bending	1579.5	1560.3	1.3485	1.3627	1.0042	1.0045
$Sm(H_2O)_2$	HOH str	3640.1	3479.0	1.3596	1.3879	1.0020	1.0020
	H_2O bending	1575.2	1547.7	1.3478	1.3625	1.0043	1.0045
HSmOH	Sm−H str	1184.3	1154.7	1.4000	1.4082	1.0000	1.0000
	Sm−OH str	510.3	495.4	1.0217	1.0353	1.0491	1.0472
$Sm(OH)_2$	sym Sm−OH str	493.8	488.0	1.0209	1.0292	−	1.0518
	asym Sm−OH str	475.3	462.1	1.0219	1.0270	1.0474	1.0467

[a] The experimental frequencies and ratios are also listed for comparison.

TABLE 6: Calculated Vibrational Frequencies (cm^{-1}) and Isotopic Frequency Ratios of the Eu + H_2O Reaction Products[a]

		freq		H/D		$^{16}O/^{18}O$	
molecule	mode	calcd	obsd	obsd	calcd	obsd	calcd
$Eu(H_2O)$	sym HOH str	3633.0	3510.8	−	1.3881	1.0017	1.0020
	H_2O bending	1582.4	1562.5	−	1.3627	1.0040	1.0044
$Eu(H_2O)_2$	HOH str	3637.9	3484.8	−	1.3880	1.0021	1.0021
	H_2O bending	1576.0	1549.0	−	1.3629	1.0043	1.0044
HEuOH	Eu−H str	1193.1	1157.0	1.3992	1.4085	1.0004	1.0001
	Eu−OH str	514.5	494.4	1.0206	1.0331	1.0490	1.0485
$Eu(OH)_2$	sym Eu−OH str	503.4	487.1	−	1.0307	1.0530	1.0514
	asym Eu−OH str	481.3	461.7	1.0226	1.0295	1.0472	1.0459

[a] The experimental frequencies and ratios are also listed for comparison.

A weak absorption at 1562.3 cm^{-1} was produced only on high-temperature annealing. The band position and isotopic shifts (Table 1) indicate that it is due to a H_2O bending vibration. The mixed $H_2{}^{16}O + H_2{}^{18}O$ spectra indicate that only one H_2O subunit is involved. This absorptions are tentatively assigned to the $Nd_2(H_2O)$ complex.

The 518.7 cm^{-1} absorption is also due to a Nd−OH stretching vibration. The mixed spectra suggest that only one OH unit is involved. This band is tentatively assigned to the NdOH molecule. DFT calculations predicted the NdOH molecule to have a $^6\Sigma$ ground state with a linear structure. The Nd−OH stretching vibration was predicted at 522.7 cm^{-1}.

Reaction Mechanism. The laser-evaporated lanthanide metal atoms (Nd, Sm, Eu) reacted with water molecules in solid argon to form the metal−water complexes and the HMOH insertion molecules. The initial step of M + H_2O reactions is the formation of the metal−water complexes, reactions 1−3:

$$Nd\ (^5I) + H_2O\ (^1A_1) \rightarrow Nd(H_2O)\ (^5A_1) \qquad \Delta E = -8.8\ \text{kcal/mol} \quad (1)$$

$$Sm\ (^7F) + H_2O\ (^1A_1) \rightarrow Sm(H_2O)\ (^7A_2) \qquad \Delta E = -9.8\ \text{kcal/mol} \quad (2)$$

$$Eu\ (^8S) + H_2O\ (^1A_1) \rightarrow Eu(H_2O)\ (^8A_2) \qquad \Delta E = -7.5\ \text{kcal/mol} \quad (3)$$

These association reactions were predicted to be exothermic by 8.8, 9.8, and 7.5 kcal/mol, respectively, after zero-point energy and basis set superposition error corrections. The $M(H_2O)$ complex absorptions increased on annealing, suggesting that reactions 1−3 require negligible activation energy. Upon sample annealing, the $M(H_2O)_2$ absorptions increased at the expense of the $M(H_2O)$ absorptions, indicating that the $M(H_2O)$ complexes further reacted with water molecules to form the $M(H_2O)_2$ complexes, reactions 4−6, which were predicted to be exothermic:

$$Nd(H_2O)\ (^5A_1) + H_2O\ (^1A_1) \rightarrow Nd(H_2O)_2\ (^5A_1) \qquad \Delta E = -13.4\ \text{kcal/mol} \quad (4)$$

$$Sm(H_2O)\ (^7A_2) + H_2O\ (^1A_1) \rightarrow Sm(H_2O)_2\ (^7A_2) \qquad \Delta E = -10.5\ \text{kcal/mol} \quad (5)$$

$$Eu(H_2O)\ (^8A_2) + H_2O\ (^1A_1) \rightarrow Eu(H_2O)_2\ (^8A_2) \qquad \Delta E = -9.9\ \text{kcal/mol} \quad (6)$$

The $M(H_2O)$ complex absorptions disappeared upon $\lambda > 500$ nm irradiation, during which the HMOH absorptions increased. The HMOH insertion molecules are formed by isomerization reactions 7−9:

$$Nd(H_2O)\ (^5A_1) \rightarrow HNdOH\ (^5A') \qquad \Delta E = -29.8\ \text{kcal/mol} \quad (7)$$

$$Sm(H_2O)\ (^7A_2) \rightarrow HSmOH\ (^7A'') \qquad \Delta E = -21.9\ \text{kcal/mol} \quad (8)$$

$$Eu(H_2O)\ (^8A_2) \rightarrow HEuOH\ (^8A'') \qquad \Delta E = -22.3\ \text{kcal/mol} \quad (9)$$

These hydrogen atom transfer processes are exothermic but require activation energies. The reactions were predicted to proceed via a transition state. The barrier heights were estimated to be 16.8, 18.9, and 19.7 kcal/mol for $Nd(H_2O)$, $Sm(H_2O)$, and $Eu(H_2O)$, respectively. Therefore, the isomerization reactions proceed experimentally under red light irradiation, during which some excited electronic states may be involved. The HNdOH absorptions also increased on annealing due to the red irradiation from the IR spectrometer which can induce isomerization. The HMOH absorptions decreased on $250 < \lambda < 580$

nm irradiation, while the metal monoxide absorptions increased. This observation suggests that the HMOH molecules rearranged to MO and H_2. In previous gas phase investigations on the reactions of metal cations with water, formation of the metal monoxide cation is the dominant reaction channel, which is proposed to proceed via the $M(H_2O)^+$ and $HMOH^+$ intermediates.[4,5,14−16]

The observation of the $M(H_2O)$ complexes is different from the early transition metal and water reactions.[7,9,10] Although the $M(H_2O)$ complexes (M = early transition metal Sc, Ti, V, etc.) were also predicted to be stationary point on the potential energy surfaces, the transition state from the complex to the HMOH insertion molecule lies lower in energy than the reactants: ground state metal atom and water; hence, the $M(H_2O)$ complex is a short-lived species, it rapidly rearranges to the HMOH insertion molecule. In the cases of Nd, Sm, and Eu, the transition states lie about 10 kcal/mol above the ground state metal atoms and water.

The absorptions due to $Nd(H_2O)_2$ also disappeared on $\lambda > 500$ nm irradiation, during which the $HNd(OH)_2$ absorptions markedly increased. It appears that red light initiates reaction 10, which was predicted to be exothermic by 10.1 kcal/mol. The reaction may also proceed via the initial formation of $Nd(OH)_2$, which then combines with H atom in the matrix to form $HNd(OH)_2$. In the Sm and Eu systems, the $Sm(H_2O)_2$ and $Eu(H_2O)_2$ absorptions also were destroyed under $\lambda > 500$ nm irradiation, during which the $Sm(OH)_2$ and $Eu(OH)_2$ absorptions increased. The experimental observation suggests that the $Sm(H_2O)_2$ and $Eu(H_2O)_2$ complexes decomposed to form $Sm(OH)_2$ and $Eu(OH)_2$, reactions 11 and 12:

$$Nd(H_2O)_2\ (^5A_1) \rightarrow HNd(OH)_2\ (^4A') + H\ (^2S) \qquad \Delta E = -10.1\ \text{kcal/mol} \quad (10)$$

$$Sm(H_2O)_2\ (^7A_2) \rightarrow Sm(OH)_2\ (^7A_2) + H_2\ (^1\Sigma_g^+) \qquad \Delta E = -50.6\text{kcal/mol} \quad (11)$$

$$Eu(H_2O)_2\ (^8A_2) \rightarrow Eu(OH)_2\ (^8A_2) + H_2\ (^1\Sigma_g^+) \qquad \Delta E = -47.9\ \text{kcal/mol} \quad (12)$$

It is interesting to note that the trivalent $HNd(OH)_2$ molecule was formed in the Nd system, whereas the divalent $Sm(OH)_2$ and $Eu(OH)_2$ molecules were observed in the Sm and Eu reactions. The 4f shell of lanthanide metals is well inside the 5d and 6s orbitals and core-like, and it generally does not involve in bonding. However, the 4f electron of Nd can be easily excited into the 5d orbital; the energy gap between the ^5I ground state with $4f^45d^06s^2$ configuration and the first excited state with $4f^35d^16s^2$ configuration is only about 19.3 kcal/mol;[27] therefore, Nd is a typical lanthanide metal exhibiting a formal oxidation state of +3. The f to d excitation energies for Sm and Eu are 75.1 and 79.6 kcal/mol,[27] respectively, which are significantly larger than that of Nd, and make them difficult to form trivalent species.

Conclusions

The reactions of early lanthanide metal atoms Nd, Sm, and Eu with water molecules have been investigated using matrix isolation infrared spectroscopy and density functional calculations. The $M(H_2O)$ and $M(H_2O)_2$ (M = Nd, Sm, Eu) metal−water complexes were produced spontaneously on annealing. The $M(H_2O)$ complexes were predicted to have planar structures which correlate to the ground state metal atoms. These 1:1 complexes rearrange to the more stable HMOH insertion isomers under red light irradiation, which could further decompose to give the metal monoxides upon UV light irradiation. Under red light irradiation, the $Nd(H_2O)_2$ complex decomposes to form the trivalent $HNd(OH)_2$ molecule, while the $Sm(H_2O)_2$ and $Eu(H_2O)_2$ complexes decompose to the divalent $Sm(OH)_2$ and $Eu(OH)_2$ molecules. In addition, HNdO and NdOH were also observed and identified.

Acknowledgment. This work is supported by NKBRSF (2004CB719501) and NNSFC (20433080).

Supporting Information Available: The calculated vibrational frequencies and intensities, and the mixed isotopic spectra. This material is available free of charge via the Internet at http://pubs.acs.org.

References and Notes

(1) Liu, K.; Parson, J. M. *J. Chem. Phys.* **1978**, *68*, 1794.
(2) Tilson, J. L.; Harrison, J. F. *J. Phys. Chem.* **1991**, *95*, 5097.
(3) Guo, B. C.; Kerns, K. P.; Castleman, A. W. *J. Phys. Chem.* **1992**, *96*, 4879.
(4) (a) Clemmer, D. E.; Aristov, N.; Armentrout, P. B. *J. Phys. Chem.* **1994**, *98*, 6522. (b) Chen, Y. M.; Clemmer, D. E.; Armentrout, P. B. *J. Phys. Chem.* **1994**, *98*, 11490.
(5) (a) Irigoras, A.; Fowler, J. E.; Ugalde, J. M. *J. Phys. Chem. A* **1998**, *102*, 293. (b) Irigoras, A.; Fowler, J. E.; Ugalde, J. M. *J. Am. Chem. Soc.* **1999**, *121*, 574. (c) Irigoras, A.; Fowler, J. E.; Ugalde, J. M. *J. Am. Chem. Soc.* **1999**, *121*, 8549. (d) Irigoras, A.; Fowler, J. E.; Ugalde, J. M. *J. Am. Chem. Soc.* **2000**, *122*, 114.
(6) (a) Rosi, M.; Bauschlicher, C. W., Jr. *J. Chem. Phys.* **1989**, *90*, 7264. (b) Rosi, M.; Bauschlicher, C. W., Jr. *J. Chem. Phys.* **1990**, *92*, 1876.
(7) Kauffman, J. W.; Hauge, R. H.; Margrave, J. L. *J. Phys. Chem.* **1985**, *89*, 3541.
(8) Kauffman, J. W.; Hauge, R. H.; Margrave, J. L. *J. Phys. Chem.* **1985**, *89*, 3547.
(9) (a) Zhang, L. N.; Dong, J.; Zhou, M. F. *J. Phys. Chem. A* **2000**, *104*, 8882. (b) Zhang, L. N.; Shao, L. M.; Zhou, M. F. *Chem. Phys.* **2001**, *272*, 27.
(10) (a) Zhou, M. F.; Zhang, L. N.; Dong, J.; Qin, Q. Z. *J. Am. Chem. Soc.* **2000**, *122*, 10680. (b) Zhou, M. F.; Dong, J.; Zhang, L. N.; Qin, Q. Z. *J. Am. Chem. Soc.* **2001**, *123*, 135.
(11) (a) Zhou, M. F.; Zhang, L. N.; Shao, L. M.; Wang, W. N.; Fan, K. N.; Qin, Q. Z. *J. Phys. Chem. A* **2001**, *105*, 5801. (b) Zhang, L. N.; Zhou, M. F.; Shao, L. M.; Wang, W. N.; Fan, K. N.; Qin, Q. Z. *J. Phys. Chem. A* **2001**, *105*, 6998.
(12) Siegbahn, P. E. M.; Blomberg, M. R. A.; Svensson, M. *J. Phys. Chem.* **1993**, *97*, 2564.
(13) Ye, S. *Theochem.* **1997**, *417*, 157.
(14) Armentrout, P. B.; Beauchamp, J. L. *Chem. Phys.* **1980**, *50*, 27.
(15) Cornehl, H. H.; Wesendrup, R.; Diefenbach, M.; Schwarz, H. *Chem. Eur. J.* **1997**, *3*, 1083.
(16) Jackson, G. P.; King, F. L.; Goeringer, D. E.; Duckworth, D. C. *J. Phys. Chem. A* **2002**, *106*, 7788.
(17) Liang, B. Y.; Andrews, L.; Li, J.; Bursten, B. E. *J. Am. Chem. Soc.* **2002**, *124*, 6723.
(18) Liang, B. Y.; Hunt, R. D.; Kushto, G. P.; Andrews, L. Li, J.; Bursten, B. E. *Inorg. Chem.* **2005**, *44*, 2159.
(19) Parker, D.; Dickins, R. S.; Puschmann, H.; Crossland, C.; Howard, J. A. K. *Chem. Rev.* **2002**, *102*, 1977.
(20) (a) Chen, M. H.; Wang, X. F.; Zhang, L. N.; Yu, M.; Qin, Q. Z. *Chem. Phys.* **1999**, *242*, 81. (b) Wang, G. J.; Gong, Y.; Chen, M. H.; Zhou, M. F. *J. Am. Chem. Soc.* **2006**, 128, 5974.
(21) (a) Becke, A. D. *J. Chem. Phys.* **1993**, *98*, 5648. (b) Lee, C.; Yang, E.; Parr, R. G. *Phys. Rev. B* **1988**, *37*, 785.
(22) (a) McLean, A. D.; Chandler, G. S. *J. Chem. Phys.* **1980**, *72*, 5639. (b) Krishnan, R.; Binkley, J. S.; Seeger, R.; Pople, J. A. *J. Chem. Phys.* **1980**, *72*, 650.
(23) Dolg, M.; Stoll, H.; Preuss, H. *J. Chem. Phys.* **1989**, *90*, 1730.
(24) Frisch, M. J.; Trucks, G. W.; Schlegel, H. B.; Scuseria, G. E.; Robb, M. A.; Cheeseman, J. R.; Montgomery, J. A., Jr.; Vreven, T.; Kudin, K. N.; Burant, J. C.; Millam, J. M.; Iyengar, S. S.; Tomasi, J.; Barone, V.; Mennucci, B.; Cossi, M.; Scalmani, G.; Rega, N.; Petersson, G. A.; Nakatsuji, H.; Hada, M.; Ehara, M.; Toyota, K.; Fukuda, R.; Hasegawa, J.; Ishida, M.; Nakajima, T.; Honda, Y.; Kitao, O.; Nakai, H.; Klene, M.; Li, X.; Knox, J. E.; Hratchian, H. P.; Cross, J. B.; Bakken, V.; Adamo, C.; Jaramillo, J.; Gomperts, R.; Stratmann, R. E.; Yazyev, O.; Austin, A. J.; Cammi, R.; Pomelli, C.; Ochterski, J. W.; Ayala, P. Y.; Morokuma, K.; Voth, G. A.; Salvador, P.; Dannenberg, J. J.; Zakrzewski, V. G.; Dapprich, S.; Daniels, A. D.; Strain, M. C.; Farkas, O.; Malick, D. K.; Rabuck, A. D.; Raghavachari, K.; Foresman, J. B.; Ortiz, J. V.; Cui, Q.; Baboul, A.

G.; Clifford, S.; Cioslowski, J.; Stefanov, B. B.; Liu, G.; Liashenko, A.; Piskorz, P.; Komaromi, I.; Martin, R. L.; Fox, D. J.; Keith, T.; Al-Laham, M. A.; Peng, C. Y.; Nanayakkara, A.; Challacombe, M.; Gill, P. M. W.; Johnson, B.; Chen, W.; Wong, M. W.; Gonzalez, C.; Pople, J. A. *Gaussian 03*, revision B.05; Gaussian, Inc.: Wallingford, CT, 2003.

(25) Willson, S. P.; Andrews, L. *J. Phys. Chem. A* **1999**, *103*, 6972.

(26) Willson, S. P.; Andrews, L. *J. Phys. Chem. A* **2000**, *104*, 1640.

(27) Martin, W. C.; Zalubas, R.; Hagan, L. *Atomic Energy Levels − The Rare Earth Elements*; Nat. Stand. Ref. Data Series, Nat. Bur. Stand. (U.S.), 1978; p 60.